Primordial features due to a step in the inflaton potential

Dhiraj Kumar Hazra[1+]**, Moumita Aich**[2†]**, Rajeev Kumar Jain**[3*]**, L. Sriramkumar**[1‡] **and Tarun Souradeep**[2§]

[1]Harish-Chandra Research Institute, Chhatnag Road, Jhunsi, Allahabad 211 019, India.
[2]IUCAA, Post Bag 4, Ganeshkhind, Pune 411 007, India.
[3]Department of Theoretical Physics, University of Geneva, 24 Quai Ernest-Ansermet, CH-1211, Geneva 4, Switzerland.

E-mail: [+]`dhiraj@hri.res.in`, [†]`moumita@iucaa.ernet.in`, [*]`rajeev.jain@unige.ch`, [‡]`sriram@hri.res.in`,[§]`tarun@iucaa.ernet.in`

Abstract. Certain oscillatory features in the primordial scalar power spectrum are known to provide a better fit to the outliers in the cosmic microwave background data near the multipole moments of $\ell = 22$ and 40. These features are usually generated by introducing a step in the popular, quadratic potential describing the canonical scalar field. Such a model will be ruled out, if the tensors remain undetected at a level corresponding to a tensor-to-scalar ratio of, say, $r \simeq 0.1$. In this work, in addition to the popular quadratic potential, we investigate the effects of the step in a small field model and a tachyon model. With possible applications to future datasets (such as PLANCK) in mind, we evaluate the tensor power spectrum exactly, and include its contribution in our analysis. We compare the models with the WMAP (five as well as seven-year), the QUaD and the ACBAR data. As expected, a step at a particular location and of a suitable magnitude and width is found to improve the fit to the outliers (near $\ell = 22$ and 40) in all these cases. We point out that, if the tensors prove to be small (say, $r \lesssim 0.01$), the quadratic potential and the tachyon model will cease to be viable, and more attention will need to be paid to examples such as the small field models.

PACS numbers: 98.80.Cq, 98.70.Vc, 04.30.-w

1. Outliers, inflationary models with a step, and tensors

Inflation continues to remain the most promising paradigm for describing the origin of the perturbations in the early universe. It has been performing remarkably well against the observational data, and the challenge before the other competing scenarios is to match the simplicity and efficiency of inflation. Many models of inflation lead to an epoch of slow roll lasting for, say, 50-60 e-folds, as is required to resolve the horizon problem. It is well known that slow roll inflation leads to a featureless, nearly scale invariant, power law, primordial scalar spectrum. Such a spectrum, along with the assumption of a spatially flat, concordant ΛCDM background cosmological model, provides a good fit to the recent observations of the anisotropies in the Cosmic Microwave Background (CMB) by different missions such as the Wilkinson Microwave Anisotropy Probe (WMAP) [1, 2], the QUEST at DASI (QUaD) [3], and the Arcminute Cosmology Bolometer Array Receiver (ACBAR) [4].

The efficacy of the inflationary scenario also seems to be responsible for an important drawback. Though, as a paradigm, inflation can be considered to be a success, it would be fair to say that we are rather far from converging on a specific model or even a class of models of inflation. There exist a plethora of inflationary models that remain consistent with the data. We mentioned above that a nearly scale invariant, power law, scalar spectrum fits the observations of the anisotropies in the CMB quite well. However, there exist a few data points at the lower multipoles—notably, at the quadrapole ($\ell = 2$) and near the multipole moments of $\ell = 22$ and 40—which lie outside the cosmic variance associated with the power law primordial spectrum. Needless to add, statistically, a few outliers in a thousand or so data points can always be expected. These outliers were noticed in the WMAP first-year data, and they continue to be present even in the most recent, seven-year data, making them unlikely to be artifacts of data analysis. It is possible that they actually indicate certain non-trivial inflationary dynamics. In that case, these outliers are important from the phenomenological perspective of attempting to constrain the models from the data, because only a more restricted class of inflationary models can be expected to provide an improved fit to these outliers. Therefore, it is a worthwhile exercise to systematically explore models that lead to specific deviations from the standard power law, inflationary perturbation spectrum, and also provide an improved fit to the data.

Various efforts towards a model independent reconstruction of the primordial spectrum from the observed pattern of the CMB anisotropies seem to indicate the presence of certain features in the spectrum [5]. (However, we should add that there also exist other views on the possibility of features in the primordial spectrum; in this context, see, for example, Refs. [6].) In particular, a burst of oscillations in the primordial spectrum seems to provide a better fit to the CMB angular power spectrum near the multipole moments of $\ell = 22$ and 40. Generating these oscillations requires a short period of deviation from slow roll inflation [7, 8], and such a departure has often been achieved by introducing a small step in the popular, quadratic potential

describing the canonical scalar field (see Refs. [9, 10, 11, 12]; for a discussion on other models, see, for instance, Refs. [13, 14]). At the cost of three additional parameters which characterize the location, the height and the width of the step, it has been found that this model provides a considerably better fit to the CMB data with the least squares parameter χ^2_{eff} typically improving by about 7, when compared to the nearly scale invariant spectrum that would have resulted in the absence of the step [11, 12]. But, such a chaotic inflation model leads to a reasonable amount of tensors, and these models will be ruled out if tensors are not detected corresponding to a tensor-to-scalar ratio of, say, $r \simeq 0.1$.

Our aims in this paper are twofold. Firstly, we wish to examine whether, with the introduction of a step, other inflationary models too perform equally well against the CMB data, as the quadratic potential does. Secondly, we would also like to consider a model that leads to a tensor-to-scalar ratio of $r < 0.1$, so that suitable alternative models exist if the tensor contribution turns out to be smaller. Motivated by these considerations, apart from revisiting the popular quadratic potential, we shall investigate the effects of the step in a small field model (in this context, see, for example, Ref. [15]) and a tachyon model [16]. Also, with possible applications to future datasets in mind (such as the ongoing PLANCK mission [17]), we shall evaluate the tensor power spectrum exactly, and include its contribution in our analysis. We shall compare the models with the CMB data from the WMAP, the QUaD and the ACBAR missions. We shall consider the five as well as the seven-year WMAP data [1, 2], the QUaD June 2009 data [3] and the ACBAR 2008 data [4] to arrive at the observational constraints on the inflationary parameters. We find that, as one may expect, a step at a suitable location and of a certain magnitude and width improves the fit to the outliers (near $\ell = 22$ and 40) in all the cases. We point out that, if the amplitude of the tensors prove to be small, the quadratic potential and the tachyon model will become inviable, and we will have to turn our attention to examples such as the small field models.

The remainder of this paper is organized as follows. In the following section, we shall outline the different inflationary models that we shall be considering in this work. In Section 3, we shall discuss the methodology that we adopt for comparing the inflationary models with the data, the datasets that we use for our analysis, and the priors on the various parameters that we work with. In Section 4, we shall present the results of our comparison of the theoretical CMB angular power spectra that arise from the various models with the WMAP five-year as well as seven-year data, the QUaD and the ACBAR data. We shall tabulate the best fit values that we obtain on the background cosmological parameters and the parameters describing the inflationary models. We shall also illustrate the constraints that we arrive at on the parameters describing the step in the case of the small field model. Further, we shall explicitly show that the models with the step perform better against the data because of the fact that they lead to an improvement in the fit to the outliers around $\ell = 22$ and 40. In Section 5, we shall illustrate the scalar power spectra and the CMB angular power spectra corresponding to the best fit values of the parameters of some of the models that we consider. Finally,

in Section 6, we shall close with a brief summary, and a few comments on certain implications of our results.

Note that we shall work in units such that $\hbar = c = (8\,\pi\,G) = 1$. Moreover, we shall assume the background cosmological model to be the standard, spatially flat, ΛCDM model.

2. The inflationary models of our interest

In this section, we shall list the different inflationary models that we shall consider, and briefly outline the parameters involved in each of these cases.

2.1. The conventional, power law case

When the tensor perturbations are also taken into account, the power law, scalar and tensor spectra are written as (see, for example, Refs. [18, 19])

$$\mathcal{P}_{\mathrm{S}}(k) = A_{\mathrm{S}} \left(\frac{k}{k_0}\right)^{n_{\mathrm{S}}-1} \quad \text{and} \quad \mathcal{P}_{\mathrm{T}}(k) = A_{\mathrm{T}} \left(\frac{k}{k_0}\right)^{n_{\mathrm{T}}}, \tag{1}$$

respectively. The quantities A_{S} and A_{T} denote the amplitude of the scalar and tensor spectra, while n_{S} and n_{T} denote the corresponding spectral indices. The quantity k_0 is the pivot scale at which the amplitudes of the power spectra are quoted. It is this power law case that will act as our reference model with respect to which we shall compare the performance of the other models against the data.

Given the scalar and tensor spectra, i.e. $\mathcal{P}_{\mathrm{S}}(k)$ and $\mathcal{P}_{\mathrm{T}}(k)$, the tensor-to-scalar ratio is defined as

$$r(k) = \frac{\mathcal{P}_{\mathrm{T}}(k)}{\mathcal{P}_{\mathrm{S}}(k)}. \tag{2}$$

When comparing the power law case with the observations, it is the tensor-to-scalar ratio r that is usually considered instead of the tensor amplitude A_{T}. Often, the following slow roll consistency condition is further assumed (see, for instance, Refs. [1, 2, 3, 4])

$$r = -8\,n_{\mathrm{T}}, \tag{3}$$

so that the power law case is basically described by the three parameters A_{S}, n_{S} and r. We should mention here that we shall *not* impose the above consistency condition while comparing the power law case with the data, and we shall work with all the four parameters A_{S}, n_{S}, r and n_{T}.

2.2. Canonical scalar field models

We shall work with two types of canonical scalar field models. We shall firstly revisit the large field, quadratic model described by the potential

$$V(\phi) = \frac{1}{2}\,m^2\,\phi^2, \tag{4}$$

where m represents the mass of the inflaton. The parameter m is essentially determined by the amplitude of the scalar power spectrum. To achieve the required number, say, 60 e-folds of inflation, in such a model, the field has to start at a suitably large value (in units of the Planck mass). The field rolls down the potential, and inflation ends as the field nears the minimum of the potential (see, for instance, Refs. [18, 19]).

The small field inflationary models offer an important alternative to the large field models. In fact, in certain cases, the small field models are possibly better motivated from the high energy physics perspective than the simple large field models (see, for example, Refs. [20]). Therefore, in addition to the quadratic potential mentioned above, we shall consider the small field model governed by the potential

$$V(\phi) = V_0 \left[1 - (\phi/\mu)^p\right]. \tag{5}$$

The field starts at small values in such models, and inflation is terminated naturally as the field approaches the value μ. As is well known (and, as we shall also discuss), the quadratic potential Eq. (4) leads to a tensor-to-scalar ratio of $r \simeq 0.1$ [12]. The small field model Eq. (5) can lead to a smaller tensor-to-scalar ratio for suitable values of μ and p (in this context, see Ref. [15]). Also, when $p < 4$, the model is known to result in a substantial red tilt. We find that, if we choose $p = 4$ and $\mu = 15$, the model leads to a tilt that is consistent with observations, and a tensor-to-scalar ratio of $r \simeq 0.01$. So while comparing with the data, we shall work with these specific values of p and μ, and vary V_0.

2.3. Tachyon model

Tachyonic inflationary potentials are usually written in terms of two parameters, say, λ and ϕ_*, in the following form [16]:

$$V(\phi) = \lambda\, V_1(\phi/\phi_*), \tag{6}$$

where $V_1(\phi/\phi_*)$ is a function which has a maximum at the origin and vanishes as $\phi \to \infty$. The tachyon model that we shall consider is described by the potential

$$V(\phi) = \frac{\lambda}{\cosh\left(\phi/\phi_*\right)}. \tag{7}$$

In such a potential, inflation typically occurs around $\phi \simeq \phi_*$. The field rolls down the potential, and inflation ends at suitably large values of the field. It is found that the quantity $(\lambda\,\phi_*^2)$ has to be much larger than unity to ensure that inflation lasts for a sufficiently long time [16]. We find that the amplitude of the scalar perturbations is more sensitive to ϕ_* than λ. Hence, while comparing with the data, we fix the value of λ, and vary ϕ_*. We shall set $\lambda = 8.9 \times 10^{-4}$. We shall then choose the priors on ϕ_* such that $(\lambda\,\phi_*^2)$ is relatively large in order to achieve the required duration of slow roll inflation.

2.4. Introduction of the step

Given a potential, say, $V(\phi)$, we shall introduce the step by *multiplying* the potential by the following function:

$$V_{\text{step}}(\phi) = \left[1 + \alpha \, \tanh\left(\frac{\phi - \phi_0}{\Delta\phi}\right)\right], \tag{8}$$

as is often done in the literature [9, 10, 11, 12]. It should be pointed out that the quantity α is positive in the case of the quadratic potential Eq. (4), whereas it is negative in the cases of the small field model Eq. (5) and the tachyon model Eq. (7). Evidently, α denotes the height of the step, ϕ_0 its location, and $\Delta\phi$ its width. When comparing with the data, in addition to the potential parameters, we shall vary these three parameters, along with the background cosmological parameters, to arrive at the observational constraints.

3. Methodology, datasets, and priors

We evaluate the inflationary power spectra numerically. In addition to the scalar power spectrum, we evaluate the tensor spectrum exactly, and include it in our analysis. We evaluate the spectra using a fast and accurate FORTRAN 90 code, which is divided into two parts. The first part uses the fourth order Runge-Kutta algorithm [21] to solve the background equations for the scale factor and the scalar field, using e-folds as the independent variable. The initial values of the field and its velocity (i.e. ϕ and $\dot{\phi}$) are chosen by hand, and we ensure that the field starts in a slow roll phase. As is the standard practice, we choose the initial value of the scale factor such that the pivot scale (viz. $k = 0.05 \, \text{Mpc}^{-1}$) leaves the Hubble radius at 50 e-folds before the end of the inflation [11, 12]. The second part of the code uses the Bulirsch-Stoer algorithm [21] to evolve the perturbations. We impose the standard Bunch-Davies initial conditions on the perturbations. As is usually done [9, 22, 23], the initial conditions on the modes are imposed when they are well inside the Hubble radius H^{-1} [say, when $k = (100 \, a \, H)$]. The modes are evolved until they are sufficiently outside the Hubble radius and the curvature perturbation reaches its asymptotic value [typically, this occurs when $k \simeq (10^{-5} \, a \, H)$]. The tensor perturbations are evolved in a similar fashion. We should mention here that, while the speed of propagation of the curvature perturbations induced by the canonical scalar field is a constant (and, equal to unity), it changes with time in the case of the tachyon models [16, 24]. We have carefully taken this point into account, while imposing the initial conditions on the modes as well as when evolving them from the sub-Hubble to the super-Hubble scales.

In order to arrive at the constraints on the various background cosmological parameters and the parameters describing the inflaton potential, we perform a Markov Chain Monte-Carlo sampling of the parameter space. To do so, we make use of the publicly available CosmoMC package [25, 26], which in turn uses the CMB anisotropy code CAMB [27, 28] to generate the CMB angular power spectra from the primordial

scalar and tensor spectra. We evaluate the scalar and the tensor spectra for all the modes that are required by CAMB to arrive at the CMB angular power spectra. For our analysis, we consider the following CMB datasets: the WMAP five-year [1] and seven-year data [2], the QUaD June 2009 data [3], and the the ACBAR 2008 data [4]. We have separately compared the models with the WMAP five-year and seven-year data. We have also compared the models with the WMAP five-year data along with the QUaD data, and with the QUaD as well as the ACBAR data. We have used the October 2009 version of CosmoMC (and CAMB) while comparing with the WMAP five-year and the QUaD and the ACBAR datasets. When comparing with the WMAP seven-year data, we have made use of the more recent version (i.e. the January 2010 version) of CosmoMC and CAMB.

In our analysis, we take gravitational lensing into account. Note that, to generate highly accurate lensed CMB spectra, CAMB requires $\ell_{\text{max scalar}} \simeq (\ell_{\text{max}} + 500)$, where ℓ_{max} is, say, the largest multipole moment for which the data is available. The WMAP data is available up to $\ell \simeq 1200$, the QUaD data goes up to $\ell \simeq 2000$, while the ACBAR data is available up to $\ell \simeq 2700$. So, we set $\ell_{\text{max scalar}} = 2500$ when dealing with the WMAP and the QUaD datasets and, when we include the ACBAR data, we set $\ell_{\text{max scalar}} = 3300$. Since the datasets involve rather large multipole moments (say, $\ell \gtrsim 1000$), we also take into account the Sunyaev-Zeldovich effect, and marginalize over the A_{sz} parameter. For the power law case, we set the pivot scale to be $k_0 = 0.05 \, \text{Mpc}^{-1}$ [cf. Eq. (1)]. We have made use of the publicly available WMAP likelihood code from the LAMBDA web-site [29] to determine the performance of the models against the data. We have have set the Gelman and Rubin parameter $|R - 1|$ to be 0.03 for convergence. Lastly, we should add that we have used the Gibbs option (for the CMB TT spectrum at the low multipoles) in the WMAP likelihood code to evaluate the least square parameter χ^2_{eff}.

As we had mentioned earlier, we incorporate the tensor perturbations in our analysis. Recall that, in the power law case, when the consistency condition Eq. (3) is not imposed, the tensor power spectrum is described in terms of the tensor-to-scalar ratio r and the tensor spectral index n_{T}. They need to be specified along with the scalar amplitude A_{s} and the corresponding spectral index n_{s}, in order to completely describe the primordial spectra. We should emphasize that, in the other inflationary models, once the parameters that govern the potential have been specified, no further parameters are required to describe the tensor power spectrum. The potential parameters determine the amplitude and shape of *both* the scalar and the tensor spectra.

As we mentioned, we assume the background to be a spatially flat, ΛCDM model described by the four standard parameters, viz. $(\Omega_{\text{b}} \, h^2)$ and $(\Omega_{\text{c}} \, h^2)$, which represent the baryon and CDM densities (with h being related to the Hubble parameter), respectively, the ratio of the sound horizon to the angular diameter distance at decoupling θ, and τ which denotes the optical depth to reionization. We work with the following priors on these parameters: $0.005 \leq (\Omega_{\text{b}} \, h^2) \leq 0.1$, $0.01 \leq (\Omega_{\text{c}} \, h^2) \leq 0.99$, $0.5 \leq \theta \leq 10.0$ and $0.01 \leq \tau \leq 0.8$. We should add that we keep the same priors on the background

parameters for all the models and datasets that we consider in our analysis. In Table 1, we have listed the priors that we choose on the different parameters which describe the various inflationary models that we consider.

Models	Parameter	Lower limit	Upper limit
Power law case	$\ln\left[10^{10}\,A_{\mathrm{S}}\right]$	2.7	4.0
	n_{S}	0.5	1.5
	r	0.0	1.0
	n_{T}	-0.5	0.5
Quadratic model with a step	$\ln\left[10^{10}\,m^2\right]$	-0.77	-0.58
	α	1.3×10^{-3}	1.7×10^{-3}
	ϕ_0	13.0	15.0
	$\Delta\phi$	0.015	0.03
Small field model with a step	$\ln\left[10^{10}\,V_0\right]$	1.50	1.86
	$-\alpha$	1.0×10^{-4}	2.0×10^{-4}
	ϕ_0	7.8	8.1
	$\Delta\phi$	5.0×10^{-3}	1.0×10^{-2}
Tachyon model with a step	$\ln\left[10^{10}\,\phi_*\right]$	34.506	34.518
	$-\alpha$	1.3×10^{-3}	1.9×10^{-3}
	ϕ_0	7.81×10^5	7.83×10^5
	$\Delta\phi$	340	410

Table 1. The priors on the various parameters that describe the primordial spectrum in the power law case, and the inflationary potential in all the other cases. We work with these priors when comparing the models with all the datasets.

4. Bounds on the background cosmology and the inflationary parameters

In this section, we shall present the results of our analysis. As we mentioned above, we have separately compared the models with the WMAP five-year and seven-year data. We have also compared the models with the WMAP five-year data along with the QUaD data, and with the QUaD as well as the ACBAR data. We shall tabulate below the best fit values that we arrive at on the various background and inflationary parameters for the power law case and for the inflationary models with the step. We shall also illustrate the behavior of the one-dimensional likelihoods for the three parameters (i.e. α, ϕ_0 and $\Delta\phi$) that describe the step in the case of the small field model Eq. (5). Further, we shall also provide the least squares parameter χ^2_{eff} in all the cases, viz. the power law case and the three inflationary models, with and without the step.

4.1. The best fit values and the one-dimensional likelihoods

In Tables 2 and 3, we have listed the best fit values for the various parameters in the power law case and in the three inflationary models with the step. These tables contain the results that we arrive at upon comparing the models with the WMAP five-year (denoted as WMAP-5) and seven-year (denoted as WMAP-7) data, the QUaD as well as the ACBAR data sets. Note that we have only presented the results for the power law case, and when the step Eq. (8) has been introduced in the quadratic potential Eq. (4), the small field model Eq. (5) and the tachyon model Eq. (7). We find that the values we have obtained upon comparing the power law case with the WMAP five and seven-year

data and the QUaD and the ACBAR data match well with the results quoted by the WMAP [1, 2] and the QUaD teams [3]. Also, the results for the quadratic potential with the step agree well with the results quoted in the recent work [12].

Datasets Parameters	WMAP-5	WMAP-5 + QUaD	WMAP-5 + QUaD + ACBAR	WMAP-7
$\Omega_{\mathrm{b}} h^2$	0.0232	0.0235	0.0229	0.0226
$\Omega_{\mathrm{c}} h^2$	0.1051	0.1011	0.1071	0.1108
θ	1.041	1.043	1.042	1.040
τ	0.0833	0.0957	0.0884	0.0895
$\ln \left[10^{10} A_{\mathrm{S}}\right]$	3.040	3.047	3.053	3.088
n_{S}	0.9764	0.9835	0.9677	0.9726
r	0.3841	0.4150	0.0667	0.1128
n_{T}	0.4112	0.4088	0.4109	0.3581

Table 2. The best fit values that we arrive at for the input parameters upon comparing the power law primordial spectra Eq. (1) with the WMAP five and seven-year, the QUaD and the ACBAR data sets. We should point out that the best fit values that we have arrived at on using the WMAP five and seven-year data match well with the values quoted by the WMAP teams [1, 2]. Similarly, we find that the values we have obtained upon comparing with the WMAP five-year and the QUaD and the ACBAR data are in good agreement with the results arrived at by, say, the QUaD team [3]. Note that, while the WMAP teams [1, 2] had worked with the pivot point of $k_0 = 0.002 \ \mathrm{Mpc}^{-1}$, the QUaD team had set the pivot scale to be $k_0 = 0.05 \ \mathrm{Mpc}^{-1}$, as we do. However, we should clarify that, whereas the WMAP and the QUaD teams had imposed the consistency condition Eq. (3), we have not done so in our analysis.

In Figure 1, we have plotted the likelihood curves for the parameters that characterize the step in the case of the small field model. In the figure, we have also included the one-dimensional likelihood for the ratio $(\alpha/\Delta\phi)$ of the step. (Note that, in the figure, WMAP-5 and WMAP-7 refer to the WMAP five and seven-year data, respectively.) We find that, while the data constrain the location of the step quite well in all the models, the bounds on the height and the width of the step are not equally tight. Interestingly, we find that the data constrains the ratio of the height to the width of the step fairly tightly.

4.2. The effective least squares parameter χ^2_{eff}

In Table 4, we have listed the least squares parameter χ^2_{eff} for all the different models and datasets of our interest. It is clear from the table that the presence of the step leads to a reduction in χ^2_{eff} by about 7-9 in all the three inflationary models that we have considered. Also, note that such an improvement is achieved in all the datasets that we have compared the models with.

When we compare the contribution to the χ^2_{eff} at the low multipoles (i.e. up to $\ell = 32$, see Refs. [1, 2]) from the output of the WMAP likelihood code for, say, the WMAP seven-year data, we find that the introduction of the step in the inflaton potential reduces the χ^2_{eff} for the TT data over this range by about 5-6 in all the cases. In Figure 2, we have plotted the difference in χ^2_{eff} with and without the step, as a function

Models	Datasets Parameters	WMAP-5	WMAP-5 +QUaD	WMAP-5+QUaD +ACBAR	WMAP-7
Quadratic potential with step	$\Omega_b\,h^2$	0.0228	0.0227	0.0228	0.0224
	$\Omega_c\,h^2$	0.1109	0.1091	0.1094	0.1108
	θ	1.041	1.041	1.042	1.0397
	τ	0.0814	0.0869	0.0902	0.0848
	$\ln\,|10^{10}\,m^2|$	-0.6893	-0.6849	-0.6774	-0.6717
	$\alpha\times10^4$	13.96	15.02	13.95	16.06
	ϕ_0	14.67	14.67	14.67	14.67
	$\Delta\phi$	0.0257	0.0259	0.0290	0.0311
Small field model with step	$\Omega_b\,h^2$	0.0228	0.0228	0.0229	0.0222
	$\Omega_c\,h^2$	0.1082	0.1084	0.1096	0.1114
	θ	1.041	1.041	1.042	1.038
	τ	0.0857	0.0868	0.0847	0.0813
	$\ln\,|10^{10}\,V_0|$	1.684	1.690	1.689	1.705
	$-\alpha\times10^3$	0.1153	0.1371	0.1701	0.1569
	ϕ_0	7.888	7.887	7.887	7.888
	$\Delta\phi$	0.0070	0.0076	0.0089	0.0090
Tachyon model with step	$\Omega_b\,h^2$	0.0226	0.0228	0.0227	0.0222
	$\Omega_c\,h^2$	0.1113	0.1103	0.1104	0.1129
	θ	1.040	1.041	1.042	1.039
	τ	0.0908	0.0937	0.0926	0.0829
	$\ln\,|10^{10}\,\phi_*|$	34.51	34.51	34.51	34.51
	$-\alpha$	0.0014	0.0016	0.0014	0.0015
	$\phi_0\times10^{-6}$	0.7818	0.7828	0.7826	0.7813
	$\Delta\phi$	378.8	371.9	341.1	352.4

Table 3. The best fit values for the various input parameters corresponding to the three inflationary models with the step. We should point out that the best fit values for the parameters that we have arrived at for the quadratic potential with the step and the WMAP five-year data are in good agreement with the results quoted in the recent work [12].

Datasets Models	WMAP-5	WMAP-5 +QUaD	WMAP-5+QUaD +ACBAR	WMAP-7
Power law case $(4,4)$	2658.40	2757.34	2779.12	7474.48
Quadratic potential $(1,1)$	2658.22 (-0.18)	2757.54 $(+0.20)$	2779.02 (-0.10)	7474.78 $(+0.30)$
Quadratic potential + step $(4,4)$	2651.00 (-7.40)	2750.38 (-6.96)	2771.72 (-7.40)	7466.28 (-8.20)
Small field model $(3,1)$	2658.26 (-0.14)	2757.46 $(+0.12)$	2779.06 (-0.06)	7474.78 $(+0.30)$
Small field model + step $(6,4)$	2650.96 (-7.44)	2750.26 (-7.08)	2771.92 (-7.20)	7466.00 (-8.48)
Tachyonic model $(2,1)$	2658.26 (-0.14)	2757.60 $(+0.26)$	2779.10 (-0.02)	7474.56 $(+0.08)$
Tachyonic model + step $(5,4)$	2651.14 (-7.26)	2750.50 (-6.84)	2772.06 (-7.06)	7465.92 (-8.56)

Table 4. The $\chi^2_{\rm eff}$ for the different models and datasets that we have considered. The two quantities that appear within the brackets in the leftmost column indicate the number of inflationary parameters available in the different models and the number of parameters that we have varied when comparing the models against the data, in that order. The quantities within the brackets in the remaining columns indicate the difference in the $\chi^2_{\rm eff}$ between the model and the power law case for that dataset, with a negative value indicating an improvement in the fit. Note that, as we had mentioned earlier, the Gibbs approach in the WMAP likelihood code has been used to calculate the $\chi^2_{\rm eff}$ for the CMB *TT* spectrum at the low multipoles (i.e. for $\ell < 32$) [1, 2]. Without the step, all the inflationary models perform just as well as the power law case. And, evidently, the introduction of the step reduces the $\chi^2_{\rm eff}$ by about 7-9 in *all* the cases.

of the multipoles when $\ell > 32$, for the WMAP seven-year data. We have plotted the difference in $\chi^2_{\rm eff}$ for the cases of the quadratic potential and the small field model. It is
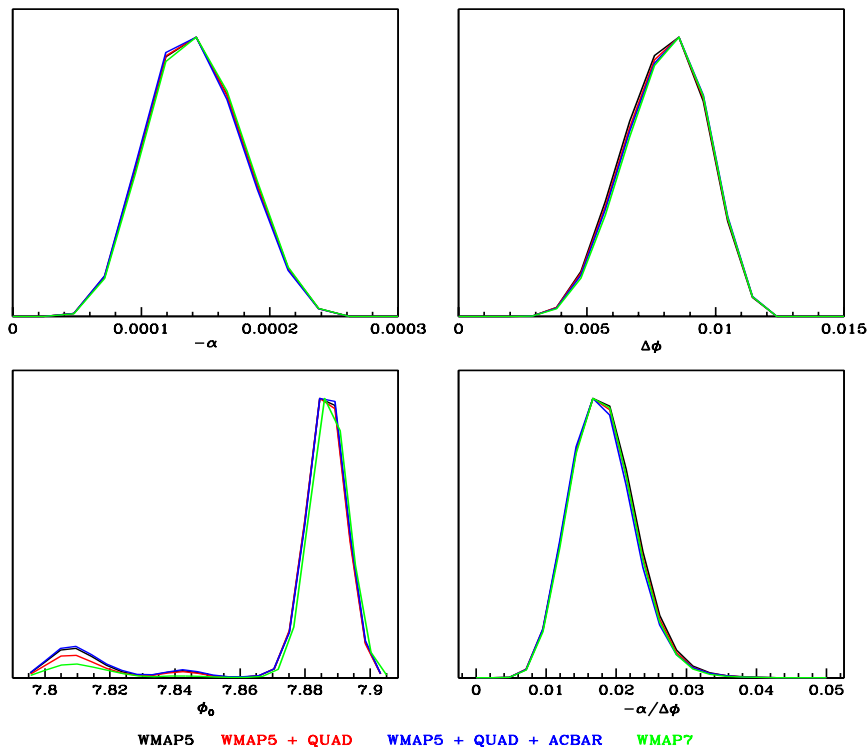
Figure 1. The one-dimensional likelihood distributions for the parameters describing the step in the case of the small field model. Note that, while the datasets strongly constrain the location of the step, the bounds are not equally tight on the height and the width of the step. However, the data seems to constain the ratio of the height to the width of the step more tightly.

clear from the figure that the additional improvement by about 2 arises due to a better fit near $\ell = 40$. (There also seems to be a 'loss' of about unity in $\chi^2_{\rm eff}$ at $\ell \lesssim 40$.) In other words, the step essentially improves the fit to the data at the lower multipoles. This point will be further evident in the following section, wherein we discuss the resulting CMB angular power spectrum.

5. The scalar and the CMB angular power spectra

As we had mentioned in the opening section, the introduction of the step leads to a small deviation from slow roll inflation [11, 12]. We have illustrated this behavior in Figure 3, wherein we have plotted the evolution of the first two slow roll parameters ϵ and η around the time when the field crosses the step in the small field model. We find that essentially the same behavior arises in all the three inflationary models that we have considered (for the definition of these slow roll parameters in the case of the canonical scalar field and the tachyon models, see, for instance, Refs. [19] and [16], respectively). The small deviation from slow roll inflation leads to a burst of oscillations superimposed
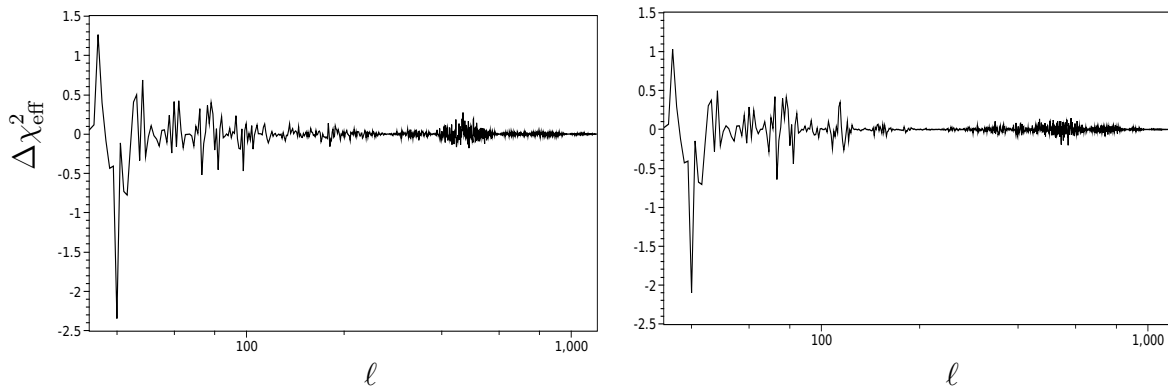
Figure 2. The difference in $\chi^2_{\rm eff}$ for the WMAP seven-year data with and without the step has been plotted as a function of the multipole moment for $\ell > 32$. The plot on the left corresponds to the quadratic potential, while the one on the right is for the small field model. The two figures are strikingly similar, and it is clear that the improvement in $\chi^2_{\rm eff}$ occurs near $\ell \simeq 40$ in both the cases. We find that the corresponding result for the tachyon model behaves in essentially the same fashion.
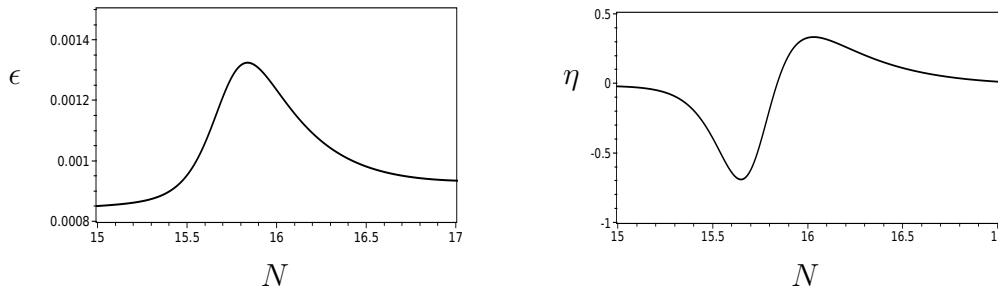
Figure 3. Typical evolution of the first two slow roll parameters ϵ and η with the introduction of the step for the three inflationary models that we have considered. We have plotted above the evolution of the slow roll parameters as a function of the e-folds N for the small field model around the time when the field crosses the step in the potential.

on the otherwise nearly scale invariant scalar power spectrum, as we have illustrated in Figure 4. We should add that, since the deviation from slow roll is relatively small, the introduction of the step hardly affects the tensor spectrum. It remains nearly scale invariant in all the cases‡. At the point $k = 0.05 \; {\rm Mpc}^{-1}$, we find the tensor-to-scalar ratio r to be about 0.16, 0.016 and 0.16 in the cases of the quadratic potential, the small field and the tachyon models, respectively.

The burst of oscillations in the scalar power spectrum in turn results in a feature in the CMB TT angular power spectrum, which leads to the improvement in the fit to

‡ We should mention that, as the effects of the step in the potential on the tensor spectrum are rather small, we could have as well worked with a suitable scale invariant amplitude for including the tensors [12].
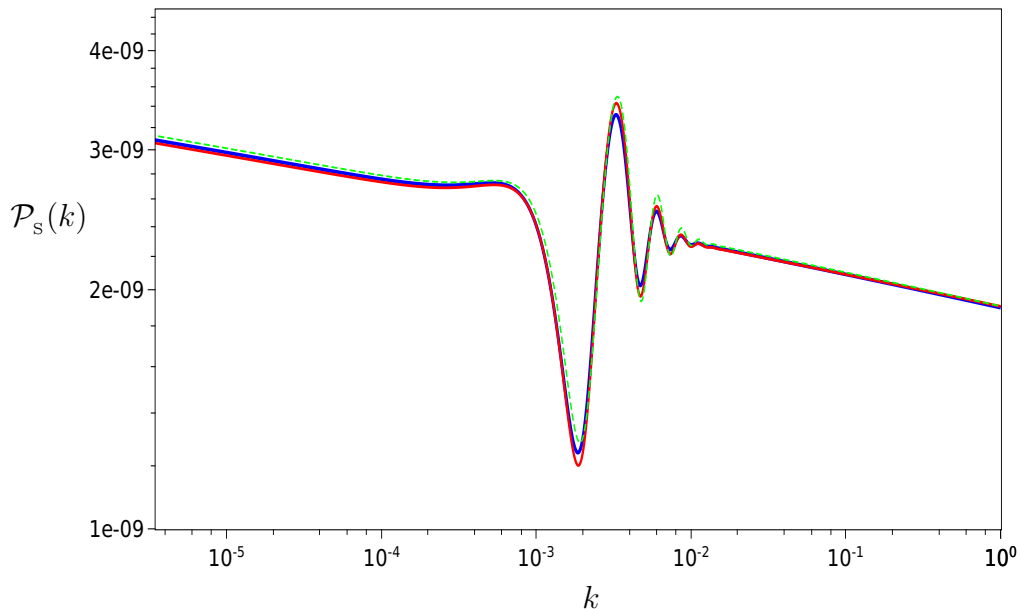
Figure 4. The scalar power spectra corresponding to the best fit values of the WMAP seven-year data for the inflationary models with the step. The solid blue, the solid red, and the dashed green curves describe the scalar power spectra in the cases of the quadratic potential, the small field model, and the tachyon model, respectively. Evidently, the three spectra are hardly distinguishable. And, obviously, the oscillations will not arise in the absence of the step.

the data at the lower multipoles. This behavior is evident in Figure 5 wherein we have plotted the CMB TT angular power spectra for the quadratic potential without and with the step, and for the small field model with the step. In Figure 6, we have plotted the corresponding TE and EE angular power spectra.

6. Summary and discussion

In this work, we have investigated the effects of introducing a step in certain inflationary models. In addition to revisiting the case of the quadratic potential that has been considered earlier, we have studied the effects of the step in a small field model and a tachyon model. The introduction of the step leads to a small deviation from slow roll inflation, which results in a burst of oscillations in the scalar power spectrum. These oscillations, in turn, leave their imprints as specific features in the CMB angular power spectrum. Actually, we have also evaluated the tensor power spectrum exactly, and have included it in our analysis. We believe that this is a timely effort considering the fact that results from, say, the ongoing PLANCK mission might necessitate such an analysis. Upon comparing the inflationary models with the WMAP, the QUaD and the ACBAR data, we find that, with the step, all the models lead to an improvement in $\chi^2_{\rm eff}$ by about 7-9 over the smooth, nearly scale invariant, slow roll spectrum, at the expense
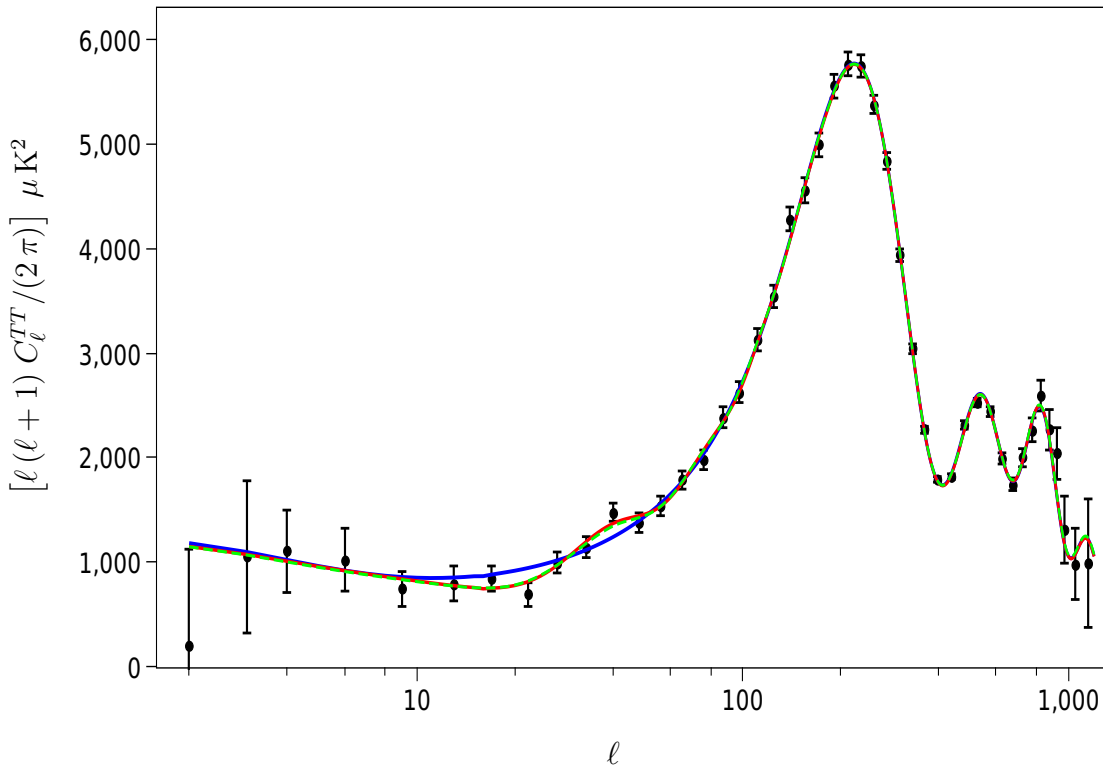
Figure 5. The CMB TT angular power spectra corresponding to the best fit values of the inflationary models for the WMAP seven-year data without and with the step. The solid blue and the solid red curves correspond to the quadratic potential without and with the step, respectively. The dashed green curve corresponds to the best fit small field model with the step. We find that the results for the tachyon model behave in exactly the same fashion. The black dots with error bars denote the WMAP seven-year data. It is visually evident that, with the introduction of the step, the models lead to a better fit to the data near the multipole moments of $\ell = 22$ and 40.

of three additional parameters describing the location, the height and the width of the step in the inflaton potential. The output of the WMAP likelihood code and a plot of the difference in χ^2_{eff} with and without the step clearly illustrate that the improvement occurs because of a better fit to the data at the lower multipoles due to the presence of the step. Evidently, if future observations indicate that the amplitude of the tensors are rather small, then the quadratic potential and the tachyon model will be ruled out, while a suitable small field model with a step can be expected to perform well against the data.

The introduction of the step in an inflationary model can possibly be viewed as an abrupt change in a potential parameter [9]. But, it has to be admitted that it is rather ad-hoc, and one needs to explore the generation of features and a resulting improvement in the fit in better motivated inflationary models. Two field models offer such a possibility. For instance, with suitably chosen parameters, the two field models
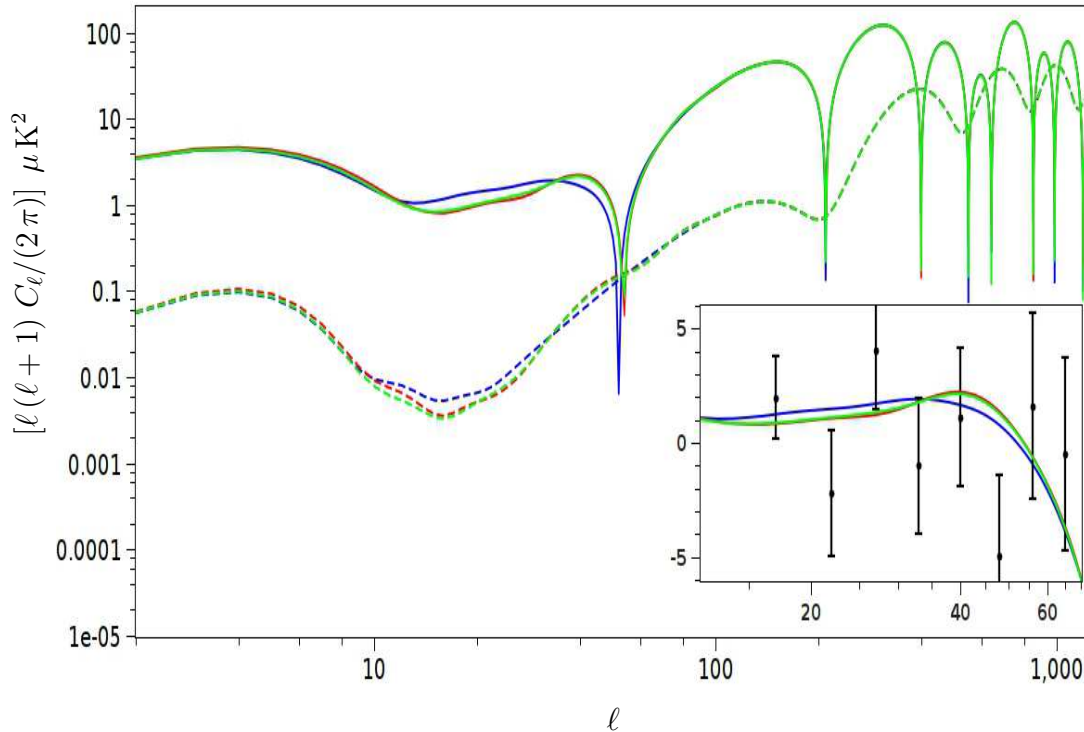
Figure 6. The CMB TE and the EE angular power spectra corresponding to the best fit values of the inflationary models for the WMAP seven-year data without and with the step. The solid blue, red and green curves represent the TE spectrum (actually, its magnitude) for the quadratic potential without and with the step, and the small field model with the step, respectively. The dashed curves denote the corresponding EE angular power spectra. The inset indicates the behavior of the TE angular power spectra against the WMAP seven-year data over the multipole interval where the discrimination is maximal.

can easily lead to a brief departure from slow roll inflation (in this context, see, for example, Refs. [13, 30, 31]). However, iso-curvature perturbations arise whenever more than one field is involved [32, 33], and they need to be carefully taken into account when comparing these models with the data. It will be a worthwhile effort to systematically explore the two field models, including the effects due to the iso-curvature perturbations, in an attempt to fit the outliers near the multipole moments of $\ell = 22$ and 40.

Over the last few years, it has been recognized that primordial non-Gaussianity can act as a powerful observational tool that can help us discriminate further between the various inflationary models. For example, it has been shown that slow roll inflation driven by the canonical scalar fields leads only to a small amount of non-Gaussianity [34]. However, recent analysis of the CMB data seem to suggest that the extent of primordial non-Gaussianity may possibly be large (see, for instance, Refs. [2, 35]). It is known that models which lead to features, such as the ones we have considered here, also generate a reasonably large non-Gaussianity (see, for example, Refs. [36]). While the

different models that we have considered in this work lead to virtually the same scalar power spectrum and almost the same extent of improvement in the fit (i.e. with the introduction of the step) to the CMB data, it is important to examine whether they lead to the same extent of non-Gaussianity as well. We are currently investigating such issues.

Acknowledgments

References

[1] J. Dunkley *et al.*, Astrophys. J. Suppl. **180**, 306 (2009); E. Komatsu *et al.*, Astrophys. J. Suppl. **180**, 330 (2009).
[2] D. Larson *et al.*, arXiv:1001.4635v1 [astro-ph.CO]; E. Komatsu *et al.*, arXiv:1001.4538v2 [astro-ph.CO].
[3] M. L. Brown *et al.*, Astrophys. J. **705**, 978 (2009).
[4] C. L. Reichardt *et al.*, Astrophys. J. **694**, 1200 (2009).
[5] S. Hannestad, Phys. Rev. D **63**, 043009 (2001); S. L. Bridle, A. M. Lewis, J. Weller and G. Efstathiou, Mon. Not. Roy. Astron. Soc. **342**, L72 (2003); P. Mukherjee and Y. Wang, Astrophys. J. **599**, 1 (2003); S. Hannestad, JCAP **0404**, 002 (2004); A. Shafieloo and T. Souradeep, Phys. Rev. D **70**, 043523 (2004); D. Tocchini-Valentini, Y. Hoffman and J. Silk, Mon. Not. Roy. Astron. Soc. **367**, 1095 (2006); A. Shafieloo, T. Souradeep, P. Manimaran, P. K. Panigrahi and R. Rangarajan, Phys. Rev. D **75**, 123502 (2007); A. Shafieloo and T. Souradeep, Phys. Rev. D **78**, 023511 (2008); R. Nagata and J. Yokoyama, Phys. Rev. D **79**, 043010 (2009); G. Nicholson and C. R. Contaldi, JCAP **0907**, 011 (2009).
[6] M. Bridges, F. Feroz, M. P. Hobson and A. N. Lasenby, Mon. Not. Roy. Astron. Soc. **400**, 1075 (2009); H. V. Peiris and L. Verde, Phys. Rev. D **81**, 021302 (2010).
[7] A. A. Starobinsky, Sov. Phys. JETP Lett. **55**, 489 (1992).
[8] C. Dvorkin and W. Hu, Phys. Rev. D **81**, 023518 (2010).
[9] J. A. Adams, B. Cresswell and R. Easther, Phys. Rev. D **64**, 123514 (2001).
[10] H. V. Peiris *et al.*, Astrophys. J. Suppl. **148**, 213 (2003).

[11] L. Covi, J. Hamann, A. Melchiorri, A. Slosar and I. Sorbera, Phys. Rev. D **74**, 083509 (2006); J. Hamann, L. Covi, A. Melchiorri and A. Slosar, Phys. Rev. D **76**, 023503 (2007).

[12] M. J. Mortonson, C. Dvorkin, H. V. Peiris and W. Hu, Phys. Rev. D **79**, 103519 (2009).

[13] M. Joy, V. Sahni, A. A. Starobinsky, Phys. Rev. D **77**, 023514 (2008); M. Joy, A. Shafieloo, V. Sahni, A. A. Starobinsky, JCAP **0906**, 028 (2009).

[14] R. K. Jain, P. Chingangbam, J.-O. Gong, L. Sriramkumar and T. Souradeep, JCAP **0901**, 009 (2009); R. K. Jain, P. Chingangbam, L. Sriramkumar and T. Souradeep, Phys. Rev. D **82**, 023509 (2010).

[15] G. Efstathiou and S. Chongchitnan, Prog. Theor. Phys. Suppl. **163**, 204 (2006).

[16] D. A. Steer and F. Vernizzi, Phys. Rev. D **70**, 043527 (2004).

[17] See, `http://www.sciops.esa.int/PLANCK/`.

[18] B. Bassett, S. Tsujikawa and D. Wands, Rev. Mod. Phys. **78**, 537 (2006).

[19] L. Sriramkumar, Curr. Sci. **97**, 868 (2009) (arXiv:0904.4584v1 [astro-ph.CO]).

[20] W. H. Kinney and K. T. Mahanthappa, Phys. Rev. D **52**, 5529 (1995); Phys. Lett. B **383**, 24 (1996).

[21] W. H. Press, S. A. Teukolsky, W. T. Vetterling and B. P. Flannery, *Numerical Recipes in FORTRAN 90*, Second edition (Cambridge University Press, Cambridge, England, 1996).

[22] D. S. Salopek, J. R. Bond and J. M. Bardeen, Phys. Rev. D **40**, 1753 (1989).

[23] C. Ringeval, Lect. Notes Phys. **738**, 243 (2008).

[24] R. K. Jain, P. Chingangbam and L. Sriramkumar, JCAP **0710**, 003 (2007).

[25] See, `http://cosmologist.info/cosmomc/`.

[26] A. Lewis and S. Bridle, Phys. Rev. D **66**, 103511 (2002).

[27] A. Lewis, A. Challinor and A. Lasenby, Astrophys. J. **538**, 473 (2000).

[28] See, `http://camb.info/`.

[29] See, `http://lambda.gsfc.nasa.gov/`.

[30] J. M. Cline, P. Crotty and J. Lesgourgues, JCAP **0309**, 010 (2003).

[31] P. Hunt and S. Sarkar, Phys. Rev. D **70**, 103518 (2004); Phys. Rev. D **76**, 123504 (2007).

[32] C. Gordon, D. Wands, B. A. Bassett and R. Maartens, Phys. Rev. D **63**, 023506 (2000).

[33] S. Tsujikawa, D. Parkinson and B. A. Bassett, Phys. Rev. D **67**, 083516 (2003); D. Parkinson, S. Tsujikawa and B. A. Bassett, Phys. Rev. D **71**, 063524 (2005).

[34] J. Maldacena, JHEP **0305**, 013 (2003).

[35] K. M. Smith, L. Senatore and M. Zaldarriaga, JCAP **0909**, 006 (2009).

[36] X. Chen, R. Easther and E. A. Lim, JCAP **0706**, 023 (2007); JCAP **0804**, 010 (2008)